

1 **Title Page**

2 **Title:**

3 Elov12 but not Elov15 is essential for the biosynthesis of docosahexaenoic acid (DHA) in zebrafish: insight
4 from a comparative gene knockout study

5 **Author:**

6 Chengjie Liu^{1,2}, Ding Ye^{1,2}, Houpeng Wang¹, Mudan He^{1,2}, Yonghua Sun^{1,2}

7 **Affiliations:**

8 1. State Key Laboratory of Freshwater Ecology and Biotechnology, Institute of Hydrobiology, Innovation
9 Academy for Seed Design, Chinese Academy of Sciences, Wuhan 430072, China.

10 2. College of Advanced Agricultural Sciences, University of Chinese Academy of Sciences, Beijing 100049,
11 China.

12 **Corresponding author:**

13 Yonghua Sun, yhsun@ihb.ac.cn

14 **ORCID of the author(s):**

15 Yonghua Sun: 0000-0001-9368-6969

16 Ding Ye: 0000-0003-3460-1122

17 **Funding:**

18 The National Key R&D Program of China (grant No 2018YFA0801000), the National Natural Science
19 Foundation of China (grant No 31972780), the Youth Innovation Promotion Association of Chinese
20 Academy of Sciences and the State Key Laboratory of Freshwater Ecology and Biotechnology (grant
21 number 2019FBZ05).

22 **Conflicts of interest:**

23 All authors report no conflicts of interest. The funders had no role in the study design, data collection, data
24 analysis and interpretation, or preparation of this manuscript.

25 **Ethics approval :**

26 The experiments involving zebrafish followed the Zebrafish Usage Guidelines of CZRC and were
27 performed under the approval of the Institutional Animal Care and Use Committee of the Institute of

28 Hydrobiology, Chinese Academy of Sciences, under protocol IHB2015-006.

29 **Authors' contributions :**

30 Y. S.: designed the study and has primary responsibility for the final content; C. L. and D. Y.: conducted
31 research; C. L., D. Y. and Y. S.: analyzed the data and wrote the manuscript; and H. W. and M. H.: provided
32 resources necessary to complete experiments. All authors read and approved the final manuscript.

33 **Abstract**

34 Teleost fish can synthesize one of the major omega-3 long-chain polyunsaturated fatty acids (n-3
35 LC-PUFAs), docosahexaenoic acid (DHA, 22:6n-3), from dietary α -linolenic acid (ALA; 18:3n-3), via
36 elongase of very long chain fatty acid (Elovl) and fatty acid desaturase (Fads). However, it remains unclear
37 which elongase is responsible for the endogenous synthesis of DHA. Here in this study, the knockout
38 models of the two major elongases, Elovl2 and Elovl5, were generated by CRISPR/Cas9 approach in
39 zebrafish and comparatively analyzed. The homozygous mutants were validated by Sanger sequencing,
40 mutation-mediated PCR and whole-mount in situ hybridization analysis of the endogenous target genes.
41 Compared with wildtype (WT) counterparts, the content of DHA was significantly reduced by 67.1%
42 ($p<0.05$) in the adult liver and by 91.7% ($p<0.01$) in the embryo at 3 day-post-fertilization (dpf) of the
43 *elovl2* mutant, but not of the *elovl5* mutant. Further study revealed that *elovl2* and *fads2* was upregulated by
44 9.9-fold ($p<0.01$) and 9.7-fold ($p<0.01$) in the *elovl5* mutant, and *elovl5* and *fads2* was upregulated by
45 15.1-fold ($p<0.01$) and 21.5-fold ($p<0.01$) in the *elovl2* mutant. Our study indicates that although both
46 Elovl2 and Elovl5 have the elongase activity toward C20, the upregulation of *elovl2* could completely
47 replace the genetic depletion of *elovl5*, but upregulation of *elovl5* could not compensate the endogenous
48 deficiency of *elovl2* in mediating DHA synthesis. In conclusion, the endogenous synthesis of DHA in is
49 mediated by Elovl2 but not Elovl5 in teleost, and a DHA-deficient genetic model of zebrafish has been
50 generated.

51 **Keywords:** Elovl2; Elovl5; docosahexaenoic acid; zebrafish

52

53 **Introduction**

54 Long-chain polyunsaturated fatty acids (LC-PUFAs), which possess 20 or more carbon atoms and contain
55 two or more double bonds in their carbon chains, e.g. docosahexaenoic acid (DHA, 22:6n-3), are essential
56 nutrients for neural development and health (Heird and Lapillonne, 2005). During the biosynthesis of
57 LC-PUFAs, fatty acid desaturase (Fads) and elongase of very long chain fatty acid (Elovl) are critical
58 enzymes for desaturation and elongation in LC-PUFA synthesis from dietary essential fatty acids,
59 α -linolenic acid (ALA, 18:3n-3) and linoleic acid (LA, 18:2n-6) (Monroig et al., 2013, Guillou et al., 2010).
60 The enzyme activities of two major elongases of different species, Elovl2 and Elovl5, have been analyzed
61 mostly in in vitro systems, such as yeast or cultured cells (Leonard et al., 2002). Functional characterization
62 assays in the yeast system revealed that the zebrafish Elovl5 and Elovl2 both have the ability to elongate
63 C18-C22 PUFA substrates (Agaba et al., 2004, Monroig et al., 2009). Although the substrate specificities of
64 Elovl2 and Elovl5 show some species-specific diversity, both Elovl2 and Elovl5 have been shown to be
65 able to elongate C20 LC-PUFA substrates (Monroig et al., 2013, Monroig et al., 2016, Monroig et al., 2012).
66 Therefore, whether the Elovl2 or Elovl5 elongase is mainly responsible for the endogenous biosynthesis of
67 DHA needs to be clarified with gene knockout models.

68 In this study, by generating *elovl2* and *elovl5* knockout zebrafish models, we revealed that Elovl2
69 dominantly mediates elongation from eicosapentaenoic acid (EPA, 20:5n-3) to DHA in teleost fish.

70

71 **Materials and Methods**

72 **Zebrafish strain**

73 Wildtype (WT) zebrafish of the AB strain were maintained and raised at the China Zebrafish Resource
74 Center of the National Aquatic Biological Resource Center (CZRC/NABRC, <http://zfish.cn>, Wuhan, China)
75 according to the Zebrafish Book (Westerfield, 2000). The adult fish were fed daily with Artemia, which
76 contain trace amounts of DHA (the LC-PUFA profile is provided in Table 1). The experiments involving
77 zebrafish followed the Zebrafish Usage Guidelines of CZRC and were performed under the approval of the
78 Institutional Animal Care and Use Committee of the Institute of Hydrobiology, Chinese Academy of
79 Sciences, under protocol IHB2015-006.

80 **Generation and identification of genetic knock-out fish**

81 Genetic mutants of *elovl2* and *elovl5* were generated by a CRISPR/Cas9-mediated knockout approach as
82 previously described (Chang et al., 2013, Ye et al., 2019). Briefly, the guide RNAs (gRNAs)
83 GGTACCGTCTTCAGTGTCAGG (PAM sequence underlined), targeting the fourth exon of *elovl2*, and
84 GGAGAAGTAATACCACCACAGG (PAM sequence underlined) targeting the fifth exon of *elovl5*, were
85 designed using CRISPRscan (<http://www.crisprscan.org/>) (Moreno-Mateos et al., 2015). The gRNAs were
86 synthesized using gRNA-pMD19-T (CZRC Plasmid #CZP3) as the PCR template according to the reported
87 method (Chang et al., 2013). The primers used for gRNAs synthesis showed in Table 2. The zebrafish
88 codon-optimized *cas9* mRNA was transcribed in vitro from pCS2-nzcas9n (CZRC Plasmid #CZP13) (Jao
89 et al., 2013). gRNA (150 pg/embryo) and *cas9* mRNA (500 pg/embryo) were co-injected into zebrafish
90 embryos at 1-cell stage as previously described (Zhang et al., 2020). The mutations were identified by
91 Sanger sequencing of the PCR products covering target sites using the primer pairs *elovl2*-testF/R and
92 *elovl5*-testF/R (Table 2). For screening of the *elovl2* and *elovl5* homozygous mutant, genomic DNA
93 extracted from zebrafish tail fin was used as a template for PCR reactions using the WT allele-specific and
94 mutant allele-specific primer pairs in Table 2 (e2F1/e2R and e2F2/e2R for *elovl2*, e5F1/e5R and e5F2/e5R
95 for *elovl5*), followed by agarose gel electrophoresis of the PCR products to identify the different genotypes.

96 **LC-PUFA analysis**

97 The livers of adult zebrafish at 3 months post-fertilization (mpf), zebrafish embryos at 3 days
98 post-fertilization (dpf) and fish diet were used for lipid extraction. The quantification of fatty acids was
99 performed by gas chromatography-mass spectrometry (GC-MS) according to our previous studies (Zhang
100 et al., 2019, Pang et al., 2014). LC-PUFAs were analyzed in three independent samples, with each sample
101 containing liver tissues of three fishes, 100 embryos or 0.1~0.2 g fish diet of brine shrimp.

102 **Whole-mount *in situ* hybridization**

103 Whole-mount *in situ* hybridization (WISH) of embryos at 3 dpf was performed as previously described (Ye
104 et al., 2019). The signal was developed by NBT-BCIP kit. Before imaging, the embryos were soaked in the
105 100% glycerol overnight at 4 °C. The images were acquired using a Leica Z16 APO microscope with a
106 Leica DFC 450FX CCD.

107 **Reverse-transcription PCR and reverse-transcription quantitative PCR**

108 RNA was extracted from livers of 3 mpf zebrafish by Trizol (Invitrogen) and the cDNA was synthesized by
109 RevertAid cDNA Synthesis Kit (Thermo). For both reverse-transcription PCR (RT-PCR) and
110 reverse-transcription quantitative PCR (RT-qPCR) analysis of *elovl2* and *elovl5*, cDNA was amplified with
111 the primers *elovl2_F/ elovl2_R* for *elovl2* (product size: 135 bp) and *elovl5_F/ elovl5_R* for *elovl5* (product
112 size: 140 bp), and *actb1* was used as the internal control. The primers were listed in Table 2. For RT-qPCR
113 analysis, real-time PCR was performed in a BioRad CFX Connect Real-Time System using SYBR Green
114 mix (BioRad) according to the MIQE (Minimum Information for Publication of Quantitative Real-Time
115 PCR Experiments) guidelines (Taylor et al., 2010). The expression levels of mRNA were calculated based
116 on the $-\Delta\Delta CT$ method according to a previous study (Pfaffl, 2001). Each RT-qPCR analysis was repeated in
117 triplicates. The primers sequences for RT-qPCR were listed in Table 2.

118 **Statistical analysis**

119 The results are expressed as the mean \pm SEM. Differences between 2 groups were tested by Student's t-test.
120 Differences were considered significant at $P < 0.05$.

121

122 **Results**

123 **Generation of zebrafish *elovl2* and *elovl5* mutants by CRISPR/Cas9**

124 The dynamic expression of *elovl2* and *elovl5* during zebrafish embryogenesis has been carefully studied
125 previously (Monroig et al., 2009). Here, we found that both genes were highly expressed in liver and
126 intestine, and they showed moderate expression levels ovary and testis of the adults (Fig. 1a). Moreover,
127 they both showed weak expression in the brain and gills, with *elovl2* showing higher expression than *elovl5*
128 in the brain, whereas *elovl5* showed higher expression than *elovl2* in the gills (Fig. 1a). By WISH analysis,
129 both *elovl2* and *elovl5* are specifically expressed in the liver primordium in the zebrafish embryos at 3 dpf
130 (Fig. 1b). These data suggested that the liver and intestine might be the main organs for LC-PUFA synthesis
131 in zebrafish.

132 To verify the in vivo function of these two elongases in fish, we then generated *elovl2* and *elovl5*
133 mutants via the CRISPR/Cas9 approach. Two alleles were generated for the *elovl2* mutants, with 20 bp

134 deletion or 2 bp deletion in the coding sequence of the elongase domain (Fig. 1c). Sanger sequencing
135 showed that the 20 bp sequence was deleted in the *elovl2* homozygous mutant (Fig. 1c). Therefore, we
136 designed WT-specific (e2F1/e2R) and mutant-specific (e2F2/e2R) primer pairs to screen the WT,
137 heterozygote and homozygote of *elovl2* mutants (Fig. 1d). In the *elovl2*^{-/-} embryo at 3 dpf, WISH analysis
138 showed that the transcription of endogenous *elovl2* totally disappeared (Fig. 1e), further indicating the
139 genetic depletion of *elovl2*.

140 Similarly, two alleles were generated for the *elovl5* mutants, with 8 bp deletion or 10 bp deletion in the
141 coding sequence of the elongase domain (Fig. 1f). Sanger sequencing confirmed that the 8 bp sequence was
142 deleted in the *elovl5* homozygous mutant (Fig. 1f). We also designed WT-specific (e5F1/e5R) and
143 mutant-specific (e5F2/e5R) primer pairs to screen the WT, heterozygote and homozygote of *elovl5* mutants
144 (Fig. 1g). WISH analysis showed that the transcription of endogenous *elovl5* totally disappeared in the
145 *elovl5*^{-/-} embryo at 3 dpf (Fig. 1h), further indicating the genetic depletion of *elovl5*. All these results
146 suggest that both genes were effectively mutated in the mutant fish and that their transcribed mRNAs
147 would be degraded due to nonsense mRNA decay mechanism (Popp and Maquat, 2016).

148 **PUFA analysis and gene expression analysis of *elovl2* and *elovl5* mutants**

149 Then we compared the fatty acids composition in the livers of WT and two mutant zebrafish at adult stage.
150 Interestingly, the amount of DHA in the liver of *elovl2*^{-/-} zebrafish (1.45±0.09%) was decreased by 67.1%
151 (p<0.05), in comparison with that in the WT (4.42±0.93%). Whereas, the amount of EPA, the synthetic
152 precursor of DHA and 22:5n-3, was increased by 48% (p<0.01) in the *elovl2*^{-/-} zebrafish (19.49±0.57%),
153 compared with that in WT (13.15±0.77%) (Fig. 2a). In contrast, there was no significant difference in the
154 contents of EPA and DHA between the WT and *elovl5*^{-/-} zebrafish (Fig. 2a). These results suggest that
155 Elovl2 plays a dominant role in endogenous synthesis of DHA, while Elovl5 is not essential for DHA
156 synthesis in zebrafish.

157 To explore the reasons for the different fatty acid composition between two mutants, we compared the
158 expression level of genes in the PUFAs synthesis pathway in the liver of WT and two mutants. Interestingly,
159 in the *elovl2*^{-/-} liver, the expression of *elovl2* was nearly absent, while the expression levels of *elovl5* and
160 *fads2* were significantly increased by 15.1-fold and 21.5-fold, respectively (Fig. 2b). Similarly, in the liver

161 of *elovl5*^{-/-} adult, expression of *elovl5* was nearly absent, while the expression levels of *elovl2* and *fads2*
162 were both increased by 9.9-fold and 9.7-fold, respectively (Fig. 2c). These results indicate that the
163 transcription of *elovl2* is activated in *elovl5* mutant and vice versa, however *elovl2* is able to fully
164 compensate the genetic loss of *elovl5*, but even high amount of Elov15 could not substitute the endogenous
165 enzyme activity of Elov12.

166 We further confirmed the role of Elov12 in the endogenous synthesis of DHA in the *elovl2*^{-/-} embryos
167 at 3 dpf, in which the content of DHA was significantly decreased by 93%, and the content of EPA was
168 significantly increased by 21% (Fig. 2d). This further validate the endogenous function of *elovl2* in the
169 embryonic developmental stage and the *elovl2*^{-/-} zebrafish is an ideal DHA-deficient model.

170

171 Discussion

172 Previous studies have shown that both fish Elov12 and Elov15 display elongation activities toward C18 and
173 C20 PUFAs in in vitro yeast system (Lebold et al., 2011, Monroig et al., 2009, Agaba et al., 2004). In our
174 study, we have utilized CRISPR/Cas9 technology to knock out both *elovl2* and *elovl5* in zebrafish, therefore
175 clearly clarify the distinct endogenous elongase activity of Elov12 and Elov15 by using those in vivo genetic
176 models. We prove that Elov12 but not Elov15 is required for endogenous conversion of C20 EPA to C22
177 docosapentaenoic acid (DPA, 22:5n-3), therefore *elovl2* mutants show deficiency of DHA synthesis.

178 In vertebrates, the endogenous synthesis of DHA may go through two alternative pathways. In
179 mammals, the endogenous synthesis of DHA is mediated by the Sprecher pathway (Sprecher, 2000), in
180 which EPA is converted to DPA and then 24:5n-3, and 24:5n-3 is subsequently desaturated and subjected to
181 chain shortening by partial β -oxidation, leading to production of DHA. Mammalian Elov12 is required for
182 elongation of DPA to 24:5n-3, thus depletion of *elovl2* in mammals led to deficiency of DHA and
183 accumulation of DPA (Gregory et al., 2013, Pauter et al., 2014). In teleost fish, however, it is proposed that
184 both the Sprecher pathway and the $\Delta 4$ pathway are active for DHA synthesis (Oboh et al., 2017, Li et al.,
185 2010). In the $\Delta 4$ pathway, DPA is directly desaturated by $\Delta 4$ desaturase to yield DHA. Unlike what was
186 observed in the *elovl2*^{-/-} mammals (Gregory et al., 2013, Pauter et al., 2014), we did not detect an
187 accumulation of DPA, the substrate of Sprecher pathway in the *elovl2*^{-/-} zebrafish. Instead, the substrate of

188 $\Delta 4$ desaturase - EPA is strongly accumulated in the *elovl2*^{-/-} zebrafish. Therefore, our study strongly
189 indicates that the $\Delta 4$ pathway should be the major pathway for endogenous synthesis of DHA in zebrafish.

190 Recent studies have established a concept of genetic compensation, in which the genetic disruption of
191 one gene might trigger the upregulation of other genes with sequence similarity, through a machinery of
192 premature termination codon (PTC) mediated nonsense mRNA decay (Ma et al., 2019, El-Brolosy et al.,
193 2019). We noticed that PTCs exist in the coding sequences of elongase domains in both *elovl2* and *elovl5*
194 mutant alleles (Fig. 1c) and both genes share high sequence similarity (data not shown), therefore the strong
195 upregulation of *elovl5* in *elovl2* mutants and vice versa were likely due to the mechanism of genetic
196 compensation in certain mutants. Given that the fatty acid profile in the *elovl5*^{-/-} liver was comparable to
197 that in WT liver, we speculated that the upregulation of *elovl2* and *fads2* in the *elovl5*^{-/-} liver could
198 completely compensate the genetic depletion of *elovl5*. However, although the *elovl2* mutant showed a
199 dramatic upregulation of *elovl5*, it still displayed a significant deficiency of DHA. This indicates that the
200 ectopically upregulated Elov5 could not replace the endogenous elongase function of Elov2 toward the
201 C20 fatty acid, EPA. All these confirm that Elov2, but not Elov5, is the main elongase for endogenous
202 synthesis of DHA from its precursor, EPA.

203 Overall, based on the present study by generating zebrafish mutants of *elovl2* and *elovl5*, both
204 endogenous Elov2 and Elov5 present elongase activity toward C18 and C20, but Elov2 is the major
205 elongase mediating the synthesis of DHA from EPA via the $\Delta 4$ pathway in zebrafish (Fig. 2e). In future, the
206 *elovl2*^{-/-} zebrafish could be used as an ideal DHA-deficient model to study the endogenous function of
207 DHA.

208

209

210 **References**

- 211 Agaba, M., Tocher, D.R., Dickson, C.A., Dick, J.R. & Teale, A.J. (2004). Zebrafish cDNA encoding
212 multifunctional fatty acid elongase involved in production of eicosapentaenoic (20:5n-3) and
213 docosahexaenoic (22:6n-3) acids. *Mar Biotechnol*, 6: 251-261.
- 214 Chang, N., Sun, C., Gao, L., Zhu, D., Xu, X., Zhu, X., Xiong, J.W. & Xi, J.J. (2013). Genome editing with
215 RNA-guided Cas9 nuclease in zebrafish embryos. *Cell Res*, 23: 465-72. DOI 10.1038/cr.2013.45
- 216 El-Brolosy, M.A., Kontarakis, Z., Rossi, A., Kuenne, C., Gunther, S., Fukuda, N., Kikhi, K., Boezio,
217 G.L.M., Takacs, C.M., Lai, S.L., Fukuda, R., Gerri, C., Giraldez, A.J. & Stainier, D.Y.R. (2019).

- 218 Genetic compensation triggered by mutant mRNA degradation. *Nature*, 568: 193-197. DOI
219 10.1038/s41586-019-1064-z
- 220 Gregory, M.K., Cleland, L.G. & James, M.J. (2013). Molecular basis for differential elongation of omega-3
221 docosapentaenoic acid by the rat Elov15 and Elov12. *Journal of Lipid Research*, 54: 2851-2857.
222 DOI 10.1194/jlr.M041368
- 223 Guillou, H., Zadavec, D., Martin, P.G.P. & Jacobsson, A. (2010). The key roles of elongases and
224 desaturases in mammalian fatty acid metabolism: Insights from transgenic mice. *Prog Lipid Res*,
225 49: 186-199. DOI 10.1016/j.plipres.2009.12.002
- 226 Heird, W.C. & Lapillonne, A. (2005). The role of essential fatty acids in development. *Annu Rev Nutr*; 25:
227 549-71. DOI 10.1146/annurev.nutr.24.012003.132254
- 228 Jao, L.E., Wentz, S.R. & Chen, W. (2013). Efficient multiplex biallelic zebrafish genome editing using a
229 CRISPR nuclease system. *Proc Natl Acad Sci U S A*, 110: 13904-9. DOI
230 10.1073/pnas.1308335110
- 231 Lebold, K.M., Jump, D.B., Miller, G.W., Wright, C.L., Labut, E.M., Barton, C.L., Tanguay, R.L. & Traber,
232 M.G. (2011). Vitamin E deficiency decreases long-chain PUFA in zebrafish (*Danio rerio*). *J Nutr*,
233 141: 2113-8. DOI 10.3945/jn.111.144279
- 234 Leonard, A.E., Kelder, B., Bobik, E.G., Chuang, L.T., Lewis, C.J., Kopchick, J.J., Mukerji, P. & Huang, Y.S.
235 (2002). Identification and expression of mammalian long-chain PUFA elongation enzymes. *Lipids*,
236 37: 733-740. DOI DOI 10.1007/s11745-002-0955-6
- 237 Li, Y., Monroig, O., Zhang, L., Wang, S., Zheng, X., Dick, J.R., You, C. & Tocher, D.R. (2010). Vertebrate
238 fatty acyl desaturase with Δ^4 activity. *Proc Natl Acad Sci U S A*. DOI 1008429107 [pii]
239 10.1073/pnas.1008429107
- 240 Ma, Z., Zhu, P., Shi, H., Guo, L., Zhang, Q., Chen, Y., Chen, S., Zhang, Z., Peng, J. & Chen, J. (2019).
241 PTC-bearing mRNA elicits a genetic compensation response via Upf3a and COMPASS
242 components. *Nature*, 568: 259-263. DOI 10.1038/s41586-019-1057-y
- 243 Monroig, O., Guinot, D., Hontoria, F., Tocher, D.R. & Navarro, J.C. (2012). Biosynthesis of essential fatty
244 acids in *Octopus vulgaris* (Cuvier, 1797): Molecular cloning, functional characterisation and tissue
245 distribution of a fatty acyl elongase. *Aquaculture*, 360: 45-53. DOI
246 10.1016/j.aquaculture.2012.07.016
- 247 Monroig, O., Lopes-Marques, M., Navarro, J.C., Hontoria, F., Ruivo, R., Santos, M.M., Venkatesh, B.,
248 Tocher, D.R. & Castro, L.F. (2016). Evolutionary functional elaboration of the Elov12/5 gene
249 family in chordates. *Scientific reports*, 6: 20510. DOI 10.1038/srep20510
- 250 Monroig, O., Rotllant, J., Sanchez, E., Cerda-Reverter, J.M. & Tocher, D.R. (2009). Expression of
251 long-chain polyunsaturated fatty acid (LC-PUFA) biosynthesis genes during zebrafish *Danio rerio*
252 early embryogenesis. *Bba-Mol Cell Biol L*, 1791: 1093-1101.
- 253 Monroig, O., Tocher, D.R. & Navarro, J.C. (2013). Biosynthesis of polyunsaturated fatty acids in marine
254 invertebrates: recent advances in molecular mechanisms. *Mar Drugs*, 11: 3998-4018. DOI
255 10.3390/md11103998
- 256 Moreno-Mateos, M.A., Vejnar, C.E., Beaudoin, J.D., Fernandez, J.P., Mis, E.K., Khokha, M.K. & Giraldez,
257 A.J. (2015). CRISPRscan: designing highly efficient sgRNAs for CRISPR-Cas9 targeting in vivo.
258 *Nat Methods*, 12: 982-8. DOI 10.1038/nmeth.3543

- 259 Oboh, A., Kabeya, N., Carmona-Antoñanzas, G., Castro, L.F.C., Dick, J.R., Tocher, D.R. & Monroig, O.
260 (2017). Two alternative pathways for docosahexaenoic acid (DHA, 22:6n-3) biosynthesis are
261 widespread among teleost fish. *Scientific Reports*, 7: 3889. DOI 10.1038/s41598-017-04288-2
- 262 Pang, S.C., Wang, H.P., Li, K.Y., Zhu, Z.Y., Kang, J.X. & Sun, Y.H. (2014). Double Transgenesis of
263 Humanized fat1 and fat2 Genes Promotes Omega-3 Polyunsaturated Fatty Acids Synthesis in a
264 Zebrafish Model. *Mar Biotechnol*, 16: 580-593.
- 265 Pauter, A.M., Olsson, P., Asadi, A., Herslof, B., Csikasz, R.I., Zdravec, D. & Jacobsson, A. (2014). Elovl2
266 ablation demonstrates that systemic DHA is endogenously produced and is essential for lipid
267 homeostasis in mice. *J Lipid Res*, 55: 718-28. DOI 10.1194/jlr.M046151
- 268 Pfaffl, M.W. (2001). A new mathematical model for relative quantification in real-time RT-PCR. *Nucleic
269 Acids Res*, 29: e45.
- 270 Popp, M.W. & Maquat, L.E. (2016). Leveraging Rules of Nonsense-Mediated mRNA Decay for Genome
271 Engineering and Personalized Medicine. *Cell*, 165: 1319-1322. DOI 10.1016/j.cell.2016.05.053
- 272 Sprecher, H. (2000). Metabolism of highly unsaturated n-3 and n-6 fatty acids. *Biochim Biophys Acta*, 1486:
273 219-31. DOI 10.1016/s1388-1981(00)00077-9
- 274 Taylor, S., Wakem, M., Dijkman, G., Alsarraj, M. & Nguyen, M. (2010). A practical approach to
275 RT-qPCR—Publishing data that conform to the MIQE guidelines. *Methods*, 50: S1.
- 276 Westerfield, M. (2000). The zebrafish book. A guide for the laboratory use of zebrafish (*Danio rerio*). 4th
277 ed.
- 278 Ye, D., Wang, X., Wei, C., He, M., Wang, H., Wang, Y., Zhu, Z. & Sun, Y. (2019). Marcksb plays a key role
279 in the secretory pathway of zebrafish Bmp2b. *PLoS genetics*, 15: e1008306. DOI
280 10.1371/journal.pgen.1008306
- 281 Zhang, F., Li, X., He, M., Ye, D., Xiong, F., Amin, G., Zhu, Z. & Sun, Y. (2020). Efficient generation of
282 zebrafish maternal-zygotic mutants through transplantation of ectopically induced and Cas9/gRNA
283 targeted primordial germ cells. *Journal of genetics and genomics = Yi chuan xue bao*, 47: 37-47.
284 DOI 10.1016/j.jgg.2019.12.004
- 285 Zhang, X.F., Pang, S.C., Liu, C.J., Wang, H.P., Ye, D., Zhu, Z.Y. & Sun, Y.H. (2019). A Novel Dietary
286 Source of EPA and DHA: Metabolic Engineering of an Important Freshwater Species Common
287 Carp by fat1-Transgenesis. *Mar Biotechnol*, 21: 171-185.
- 288

289 **Figure legends:**

290 **Fig. 1** Generation and validation of *elovl2* and *elovl5* mutant zebrafish. (a) RT-PCR analysis of *elovl2* and
291 *elovl5* in different tissues. (b) Expression patterns of *elovl5* and *elovl2* in WT embryos (3 dpf) examined by
292 WISH. The red arrows showed the signals of *elovl2* and *elovl5* in the liver primordium region. (c) Diagram
293 showing the gRNA target of *elovl2*, the genotypes and the length and structure of the predicted mutant
294 proteins. Sanger sequencing was used to detect the *elovl2* mutation type 1 with 20 bp deletion. (d)
295 Identification of WT, *elovl2* heterozygous (het), and *elovl2* homozygous (homo) fish with PCR primer pairs,
296 e2F1/e2R and e2F2/e2R. (e) Expression pattern of *elovl2* in *elovl2*^{-/-} embryos (3 dpf) examined by WISH.
297 The white arrow showed that the signal of *elovl2* was not detected in the liver primordium. (f) Diagram
298 showing the gRNA target of *elovl5*, the genotypes and the length and structure of the predicted mutant
299 proteins. Sanger sequencing was used to detect the *elovl5* mutation type 1 with 8 bp deletion. (g)
300 Identification of WT, *elovl5* heterozygous (het), and *elovl5* homozygous (homo) fish with PCR primer pairs,
301 e5F1/e5R and e5F2/e5R. (h) Expression pattern of *elovl5* in the *elovl5*^{-/-} embryos (3 dpf) examined by
302 WISH. The white arrow showed that the signal of *elovl5* was not detected in the liver primordium.

303

304 **Fig. 2** *Elovl2* but not *Elovl5* is the major elongase mediating the biosynthesis of DHA from EPA in
305 zebrafish. (a) Fatty acid composition (molecular percentage) in the livers of WT (13.15±0.77% for 20:5n-3;
306 4.42±0.93% for 22:6n-3), *elovl2*^{-/-} (19.49±0.57% for 20:5n-3; 1.45±0.09% for 22:6n-3) and *elovl5*^{-/-}
307 (13.67±0.61% for 20:5n-3; 4.70±0.28% for 22:6n-3). n = 3 replicates. (b) Relative mRNA levels of *elovl2*,
308 *elovl5* and *fads2* in the livers of WT and *elovl2*^{-/-} fish examined by RT-qPCR. n = 3 replicates. (c) Relative
309 mRNA levels of *elovl5*, *elovl2* and *fads2* in the livers of WT and *elovl5*^{-/-} fish examined by RT-qPCR. n = 3
310 replicates. (d) Fatty acid composition (molecular percentage) in the embryos of WT (5.18±0.28% for
311 20:5n-3; 3.34±0.33% for 22:6n-3) and *elovl2*^{-/-} (6.29±0.14% for 20:5n-3; 0.23±0.05% for 22:6n-3) at 3 dpf.
312 n = 3 replicates. (e) Diagram showing the biosynthetic pathway of n-6 and n-3 LC-PUFAs in WT and
313 *elovl2*^{-/-} zebrafish. The green and red texts indicate the enzyme activities are stimulated or blocked in the
314 *elovl2*^{-/-} zebrafish. The green and red arrows indicate the increase or decrease of the content of EPA and
315 DHA in *elovl2*^{-/-} zebrafish. All values are the mean ± SEM. Student's t-test was used in all panels. *, P <

316 0.05, **, $P < 0.01$, *** $P < 0.001$., and NS, no significant difference.

317 **Table 1** LC-PUFAs composition¹ of total fatty acids extracted from *Artemia*

Fatty acid	Mol% of total fatty acid
18:2n-6	6.04±0.05
18:3n-6	0.16±0.01
20:2n-6	0.19±0.01
20:3n-6	0.14±0.01
20:4n-6	2.07±0.08
22:4n-6	0.01±0.00
18:3n-3	9.60±0.02
20:5n-3	19.60±0.20
22:5n-3	0.04±0.01
22:6n-3	0.48±0.02

318 ¹ Values are means ± SEM; n = 3 samples.

319 **Table 2** List of primers used in present study

Name	Sequence (5'-3')	Objective
<i>elovl2</i> -gRNA-Forward	TAATACGACTCACTATAGGTTACCGTCTTCAGT GTCGTTTTAGAGCTAGAAATAGC	gRNA amplification
<i>elovl5</i> -gRNA-Forward	TGTAATACGACTCACTATAGGAGAAGTAATAC CACCACGTTTTAGAGCTAGAAATAGC	
gRNA- Reverse	AAAAAAAGCACCCGACTCGGTGCCAC	
<i>elovl2</i> -testF	CTCATCTGCCAATGTCGA	mutation analysis
<i>elovl2</i> -testR	TTTCATCCCAAAGCCAAG	
<i>elovl5</i> -testF	CTGGTCATGTCTGTGTATCA	
<i>elovl5</i> -testR	AGTGTCCACACGGCACCCAG	
e2F1	TTACCGTCTTCAGTGTCCAGG	mutant screening
e2F2	GCAGTCTGGTCTGCAGGCAC	
e2R	TCCTACAAACCACTTGAATGTG	
e5F1	GATGAATGTCCTGTGGTGGTAT	
e5F2	GATGATGAATGTCCTGTTAC	
e5R	TGTTGCATGTAGCAAAGCAC	
<i>elovl2</i> _F	AGTAAGCGCATGGGTGCTTC	RT-qPCR
<i>elovl2</i> _R	CCACCCTCGGTTTACCTCTTTT	
<i>elovl5</i> _F	ATCACGCCACCATGCTCAAC	
<i>elovl5</i> _R	CAAAGCTGGAACCGCAGACA	
<i>fads2</i> _F	CATTGGTCCTCCCCTGCTCA	
<i>fads2</i> _R	CGCCGTAGAACTGCGTGTA	
<i>actb1</i> -F	GATGATGAAATTGCCGCACTG	
<i>actb1</i> -R	ACCAACCATGACACCCTGATGT	

320

321

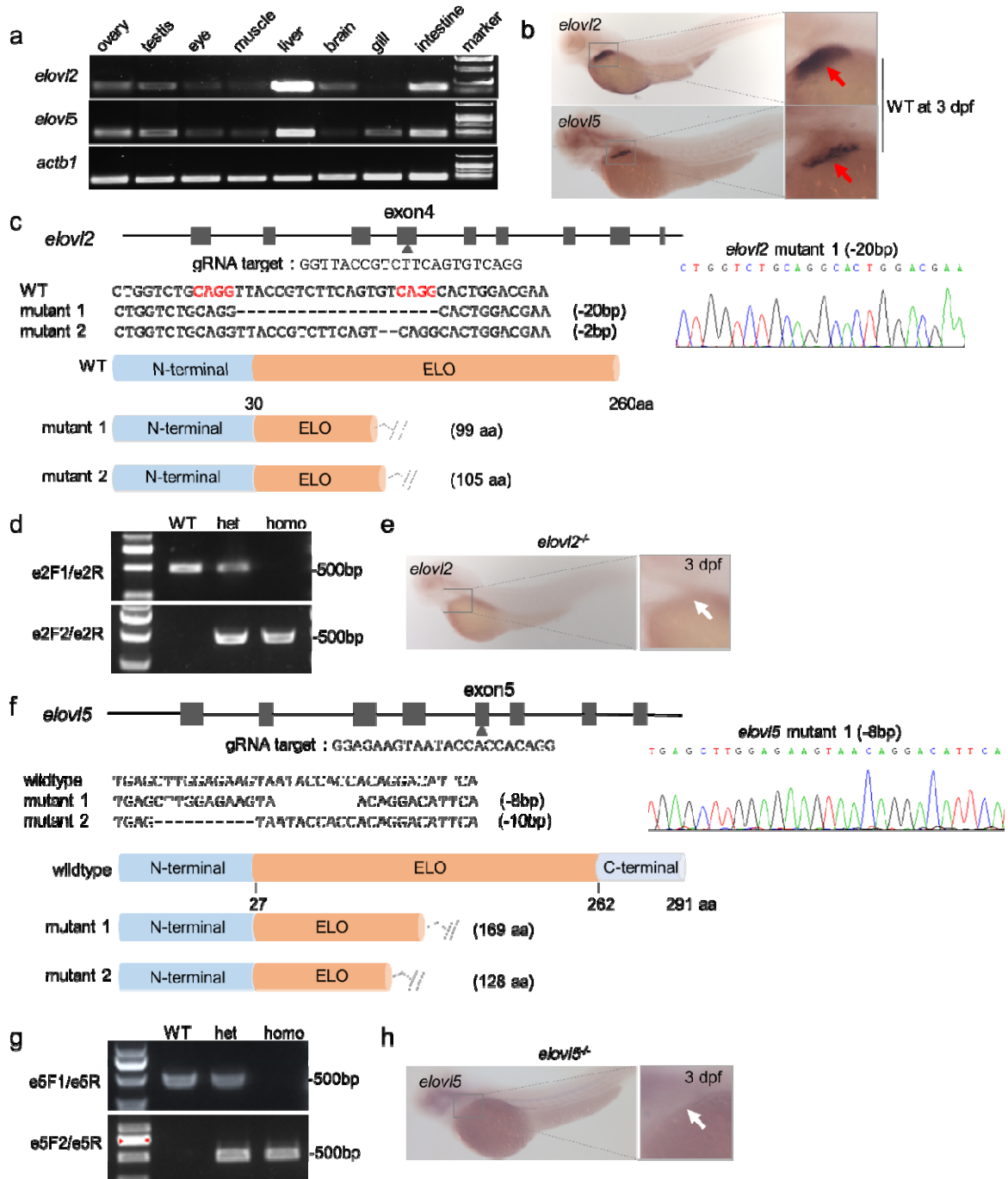
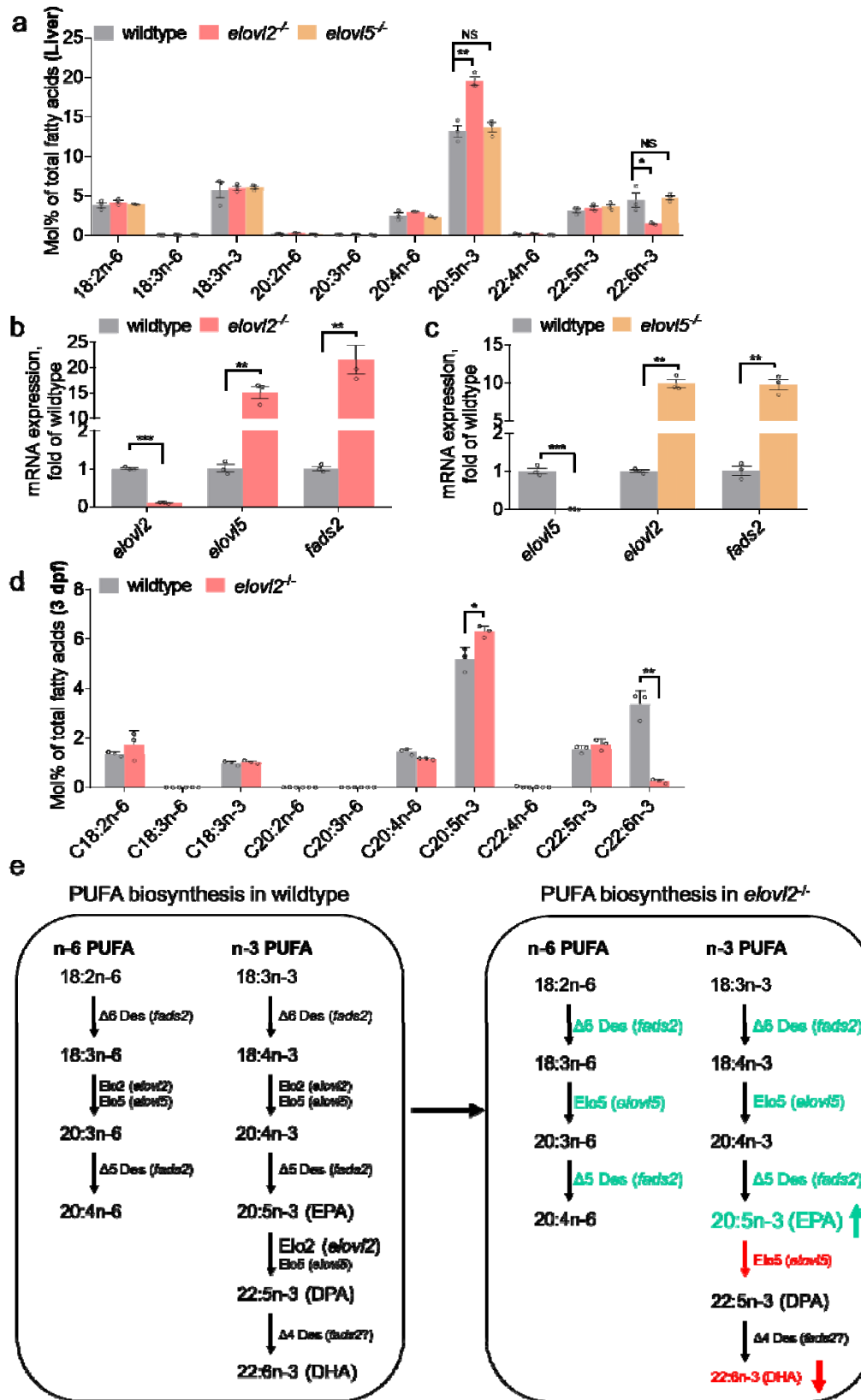


Fig. 1

322

323

324



325

326

Fig. 2